buildings

MDPI

Article

Proposed Simplified Approach for the Seismic Analysis of Multi-Storey Moment Resisting Framed Buildings Incorporating Friction Sliders

Shahab Ramhormozian [1,*], G. Charles Clifton [2], Massimo Latour [3] and Gregory A. MacRae [4]

1 Department of Built Environment Engineering, Auckland University of Technology, Auckland 1010, New Zealand
2 Department of Civil and Environmental Engineering, University of Auckland, Auckland 1010, New Zealand; c.clifton@auckland.ac.nz
3 Department of Civil Engineering, University of Salerno, 84084 Salerno, Italy; mlatour@unisa.it
4 Department of Civil and Natural Resources Engineering, University of Canterbury, Christchurch 8041, New Zealand; gregory.macrae@canterbury.ac.nz
* Correspondence: shahab.ramhormozian@aut.ac.nz; Tel.: +64-9-921-999 (ext. 7631)

Received: 29 April 2019; Accepted: 20 May 2019; Published: 23 May 2019

Abstract: An innovative, simplified, and accurate model is proposed and developed to enable simplified yet realistic time history analysis of multi-storey buildings with moment resisting connections using friction energy dissipaters in the commonly used structural analysis and design program, SAP2000. The analyses are rapid to undertake, thereby enabling detailed study of the influence of many building system effects on the overall response. This paper presents the outcome of dynamic analysis of a complete 13-storey moment resisting steel building with Sliding Hinge Joints as the beam-column connections, considering the influential self-centring factors such as MRF and gravity columns continuity as well as column base and diaphragm flexibilities. The building is one of the Te-Puni towers, which are structural steel apartment buildings with steel-concrete composite floors, designed according to the low damage design philosophy, built in Wellington, New Zealand in 2008 and which have already been subjected to two significant earthquakes. The key objectives of the research have been to take the design of the 13-storey building and convert that into the proposed simplified model required for time history seismic analysis, to undertake analysis under scaled El-Centro earthquake record, investigate the peak inter-storey drift and the residual drift of the building, and determine the influence of column base rotational stiffness, floor slab out of horizontal plane displacement, type of friction damper, and MRF and gravity column continuity. It is concluded that the response of the building is stable and predictable, as expected, and that the post-earthquake state of the building, particularly from the self-centring point of view, is well within the limits for maintaining operational continuity following an ULS level design earthquake.

Keywords: Non-Linear Time-History Analysis; Sliding Hinge Joint; Self-centring; Friction Sliding Connection; Low damage; Energy Dissipation; Seismic Design

1. Introduction

Sliding Hinge Joints (SHJ) with Asymmetric Friction Connections (SHJAFC) are connections widely used throughout New Zealand. These connections are used to connect beams to columns and are designed and detailed to be rigid up to a defined design level of earthquake demand. Once this is exceeded, the connection allows rotation of the column, relative to the beam, due to sliding in the Asymmetric Friction Connection (AFC) components which are ideally intended to seize up and become rigid again at the end of the severe shaking. See the SHJAFC layout and components in Figure 1.

The aim of this research, which was first presented [1] at the Pacific Conference on Earthquake Engineering, is to propose a simple numerical model which determines the response of the building and to analyse the performance of a complete building system implementing AFC and Symmetrical Friction Connection (SFC) through non-linear time history analysis. This research also explores the influence of several parameters and their effects on the dynamic response and residual drift of the building experiencing an actual severe earthquake excitation. These parameters include continuous elastic columns, elastic column bases, gravity columns, and floor out of plane strength and stiffness.

Objectives

The objectives of this research included:

- Converting the 13 storey Te Puni building with friction sliders into a simplified Multi Degree of Freedom (MDF) building model using SAP2000 software. This focused only the longitudinal moment resisting frame direction of the building, as the transverse direction uses rocking concentrically braced frames as the seismic-resisting system.
- Recording the dynamic response of the building using a past earthquake time-history record representative of the type of severe earthquake expected at that location to excite the building for different limit states.
- Quantifying maximum displacement values.
- Quantifying the self-centring capabilities of the structure using residual drift values from model outputs to compare SFC and AFC detailing.
- Producing recommendations if there is a need to minimize post-earthquake residual drift.
- Investigating the influence of changing column base rotational stiffness on the seismic behaviour of the building.

2. Background

Capacity design was first introduced in the late 1960s by John Hollings, [2] who proposed a hierarchy of failure within a structure. He put forward the "strong column-weak beam" inelastic design mechanism for rigid moment resisting frames that we use today. In a severe seismic event, this mechanism concentrates the inelastic demand into the beams and suppresses inelastic demand in the columns, in order to prevent a column failure and hence a storey failure. The energy from an earthquake is required to be dissipated in a manner that is dependable and stable and so, to achieve this, the plastic deformation is limited to hinges (plastic hinges). These plastic hinges need to be designed in specific locations within the structure (i.e., in the beams of a rigid moment resisting frame; this is to ensure that the plastic hinges yield in the structure first enabling the desired mechanism to be developed, before inelastic demand occurs in other components [3].

In steel buildings, moment resisting frames (MRFs) are one of the most commonly used lateral force resisting systems. MRFs resist lateral loads by the development of bending moment and shear force in the beams and columns of the MRF. In current practice, to apply the capacity design philosophy to a rigid MRF, the plastic hinges are located at the end of the beams, and the column and connections are designed to resist the capacity designed actions from the beam. This system provides safety and prevents collapse, but the issue is that in doing so it incurs irrecoverable plastic deformation in the beams or joints, necessitating post-earthquake evaluation and repair. While this is intended from the design, there are heavy economic losses associated with the repair and downtime of the building [4]. These economic losses have been experienced in recent severe earthquakes such as the 1994 Northridge, 1995 Kobe and, more recently and significantly, in the 2010/2011 Christchurch and 2016 Kaikoura earthquakes [5]. This has brought a global focus on the "development and implementation of low-damage seismic resisting systems that are able to reduce the amount of disruption caused to earthquake-affected regions" [6]. This system's aim is to have the building operating immediately or

rapidly after a major earthquake, with minimal damage and with repair able to be undertaken to suit scheduled building maintenance.

The Sliding Hinge Joint (SHJ) was developed by Charles Clifton [7], between 1998 and 2005, as a proposed solution to the need for a low-damage seismic resisting system. It is a low-damage alternative to traditional beam-column connections for seismic MRSFs (moment resisting steel frames) and has been used in several multi-storey buildings in New Zealand [5]. It is intended to serve three main functions [4]: 1) Behave rigidly under serviceability limit state conditions, 2) Behave semi-rigidly under ultimate limit state conditions and tolerate large beam-column relative rotation, 3) At the end of the earthquake, seize back up and become rigid again.

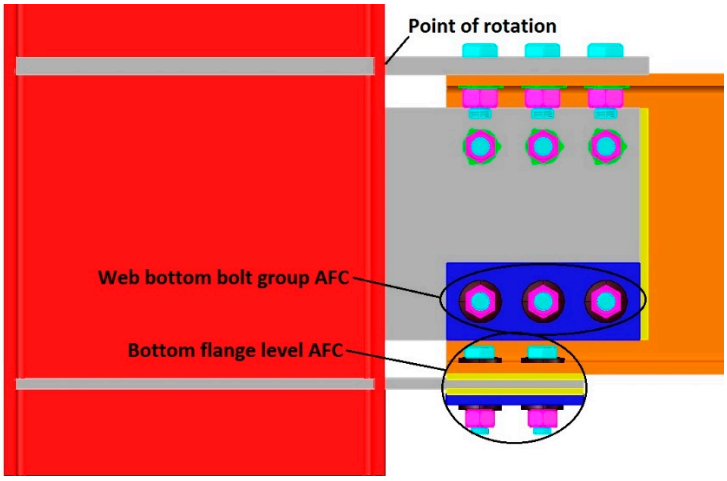

Figure 1. The SHJ layout with AFCs [6].

Figure 1 shows the SHJ with the AFCs, which are located at the bottom web and bottom flange bolt groups. It is important to note that the point of rotation for the SHJ is where the top flange plate extending from the column is bolted to the beam flange. When an increasing bending moment is subjected to the SHJ, it initially performs as a rigid connection until the moment in the beam ends exceeds the frictional resistance of both AFCs, then the connection performs as a semi-rigid connection and rotation occurs causing energy to be dissipated through friction sliding of the AFCs [8]. The AFC is comprised of a shim, cleat, another shim and the cap plate all clamped by fully tensioned high-strength friction grip bolts, according to the current New Zealand practices [9]. It offers a simple to build and cost-effective means of capably dissipating energy under the ultimate limit state and greater earthquake loading [8].

However, there are concerns with the AFC's post-sliding elastic strength reduction [9]. The originally developed AFC has been experimentally tested and it has shown that after a few cycles of significant sliding, the AFC experiences a major reduction in clamping force as a result of the bolts losing tension [5]. The sliding shear capacity is based on the stable sliding bolt tension, which is lower than the proof load to which the bolt was originally tightened. However, this loss of tension means that the AFC will commence sliding in lower intensity earthquakes following the main event, or even in significant wind loading. The only solution to this with the original AFC design is to perform time-consuming retightening of the bolts, which will be required if the earthquake is sufficiently severe.

The primary reason for bolt tension loss is because of the interaction between the bending moment, shear force and tensile force causing the bolt to partially plasticise [9]. This has highlighted the potential benefit of not yielding the bolts during their installation but installing the bolts in their elastic range which ensures the bolts have a dependable elastic deformation capacity under severe earthquakes [9]. There are two other reasons responsible for bolt tension loss; the prying of the cleat imposing a longitudinal plastic strain on the bolts during sliding and the sliding grip length being slightly shortened post sliding due to the abrasion of the surfaces [9].

Research has been undertaken on the optimal installed bolt tension to minimise post-earthquake damage and it was found that even with the optimal bolt tension, "bolts were still losing 60% of initial tension and therefore, would require retightening after the seismic event" [9]. The addition of Belleville springs (BeSs) to decrease the post-sliding tension loss has been investigated by researchers [8,10], showing that they can maintain 80% of the original installed tension [9]. This figure is important, as it is the target for retention of the original strength and stiffness set by several groups internationally studying the dynamic response of earthquake damaged and repaired buildings. The implementation of the BeSs in the AFC enables the SHJ to undergo minimal loss of strength and stiffness in a subsequent severe earthquake had has led to the design of the optimised sliding hinge joint with asymmetric friction connections [10].

Permanent horizontal displacement can occur after an earthquake and is referred to as residual drift [11]. Self-centring is the building's ability to return to its original position, with the residual drifts being within the construction tolerance limits [6]. The Belleville springs implementation in the SHJ have been found to provide considerable improvements in the joint self-centring capability [8]. The testing only included one AFC in the SHJ and the effects of a whole SHJ connection with two AFCs and additional sources of restoring energies are expected to provide further improvements to self-centring capabilities [8]. These additional sources of restoring energies include: floor slab out of plane strength and stiffness, continuous elastic columns, and elastic column bases, which are all present in a complete building.

Ramhormozian and Clifton [6] studied the static and dynamic self-centring capability of a single degree of freedom system concluding that static requirements can be significantly relaxed to make a system dynamically self-centre, hence instead of static self-centring, the dynamic self-centring capability needs to be considered while investigating the self-centring capability of a seismic resisting system. However, their study was on a SDOF only. In practice, each level of the structure is linked to other levels with columns that are designed and detailed to be elastic and continuous. Taking these conditions into account is the focus of this article.

Research undertaken by Ramhormozian and Clifton [3] included dynamic performance analysis and system identification of a multi-storey moment resisting framed building with the SHJs, undertaken on the same building as the one considered in the current paper, under two moderately severe earthquake events. This showed that the SHJs underwent measurable sliding during both earthquakes; however, the SHJs experienced no measurable loss of strength and stiffness and exhibited self-centring behaviour. However, the sliding demand was less than 10% of that generated by the component experimental testing described in [6]. This conclusion was also a driver behind the research presented in this article to numerically study and explain the actual seismic behaviour of the building.

The Te Puni Building

The Te Puni building houses students from Victoria University in Wellington, New Zealand. In the design brief, a goal of the building was to deliver a robust steel frame building that would remain operational immediately after a severe earthquake, while the rest of the University buildings are being repaired [3]. It is built on highly weathered greywacke rock with a layer of soft soil on top causing different levels of seismic acceleration than other parts of the Central Business District [12]. The building stands 11 storeys high on a 12 m by 15 m concrete slab which supports a moment resisting steel frame in the longitudinal direction with SHJs at the beam to column connections [3]. In the transverse direction, as previously noted, the Te Puni building has a concentrically braced frame with SHJs at both ends of the steel beams. Structural system selection and more structural details of the Te Puni Building may be found in [13,14].

3. Methodology

The focus of the research places great importance on the development of a simple yet representative model that encompasses all the elements expected to influence the deflection envelopes and residual

drift values after an earthquake. The modelling of the 13-storey Te Puni building using SAP2000 structural analysis software was therefore a critical objective to attain dependable results.

The following sections detail the process in developing the multi degree of freedom (MDOF) model as well as earthquake scaling procedures and detailed Non-Linear Time History Analysis (NLTHA).

3.1. Model Data Extraction

All relevant details pertaining to the building were extracted from the Te Puni calculation set produced by the Design Engineers, Connell Wagner, where information for the base skeleton model encompassing three representative columns and the SHJ detailing could be collated. The first storey above ground level was identified as Level 4 which numerically increased to Level 13 as the top storey considered in the model. It will hence be referred to as such to remain consistent with the calculation notation.

The three types of columns identified as having various base fixities and unique characteristics and therefore needing to be kept distinct in the model were the Moment Resisting Frame (MRF) columns, the Concentrically Braced Frame (CBF) columns and the gravity system columns, as shown in Figure 2. The details of interest to build the representative columns for the base skeleton of the building were Column and Beam Sizes, Stiffener and Doubler Plate Sizes, Number of Columns by Type, Slab and Deck Thickness, and Vertical Locations of Specific Features—Members, Panel Zones, Top and Bottom Stiffener Regions, Sliding Hinge Joint Connections.

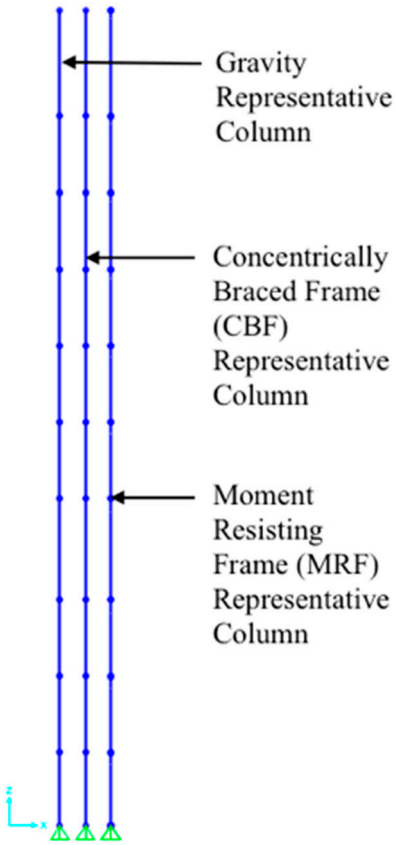

Figure 2. Representative column model placement.

The other component required to complete the representative model was the SHJ, specifically the relevant details which would later influence the definition of the link properties. This was inclusive of number, size and pitch of bolts per web connection, and number, size and pitch of bolts per flange connection.

Other features which were incorporated for capturing the behaviour of the Te Puni building, which were taken from the calculation set, included seismic weights and permanent and imposed loading.

3.2. Representative Column Base Skeleton Definition

With an initial gridline definition set in the X-Z plane, the X coordinate grid was defined for the three representative columns spaced at 1 m apart to establish the column centreline positions. The Z coordinate grid was defined based on the vertical locations, as identified within the extraction phase, so that the structural elements up the full height of 32 m can be placed at their exact locations.

All different column and beam sections were defined using AS 3679-G300 steel. While CBF and gravity representative columns were simple to establish, where each column simply connects in the model from the top of one storey to another to form a continuous member, the MRF counterpart had extra detailing which required careful definition, as seen in Figure 3. Stiffeners were defined as a rectangular plate to the thicknesses specified in the calculation set. This accounted for extra stiffness in those areas. Panel zones were defined as modified UB sections where the thickness of the web had been increased due to presence of 6 mm doubler plates on each side. The shear, stiffness and moment modifiers for all sections were changed to account for the true number of MRF, CBF and gravity columns within the Te Puni building, which were 12, 8 and 4, respectively. To avoid double counting, the mass and weight modifiers were set to 0 for all sections, as the extracted seismic weight for each floor was incorporated separately and directly into the model.

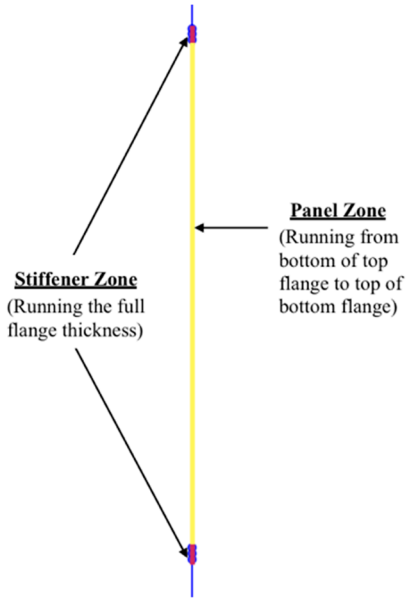

Figure 3. Column stiffener and panel zones.

Once the structural elements had been defined as above, they were drawn using the SAP2000 software from the bottom to the top of the building in their respective locations. The MRF and CBF columns were treated as having a fixed base with infinite rigidity to distribute demands almost entirely into the foundation while the gravity column is more closely represented through a pinned base where demands are instead distributed throughout the column itself. The base node of each representative column was however all assigned as pinned as the occurrence of such ideal base conditions are not realistically achieved in practice. To account for this rotational stiffness more accurately, rotational springs were applied, connecting from the first storey column to the foundation. In practice these need to follow the rotational limits stated in [15], where a pinned base assumes the lower limit ($k = 0.1 \times EI/L$), and a fixed base assumes the upper limit ($k = 1.67 \times EI/L$). To explore the effects of an intermediate type of base detailing for the MRF and CBF columns, as they may not achieve the

rigidity expressed from the upper limit, a third reduced rotational stiffness equation ($k = 1.0 \times EI/L$) may be defined to investigate the influence of drift values in the results. It is worth noting that the results presented in this article are based on the rotational stiffness of the column bases being 10% of the above-mentioned values, meaning that the column bases of the MRFs have been effectively pinned, and the column bases of the gravity columns were perfectly pinned.

While the Young's modulus of steel (E) and the length of the columns (L), being the full height of the first level column, remain the same, the moment of inertia (I) values are taken as an average for each column type. Table 1 shows the final rotational spring stiffness defined to capture the base fixity under each representative column, having applied the same aforementioned multipliers according to column type to embody the entire building.

Table 1. Rotational spring stiffness values used for base fixity model detailing (all in a range of pinned column base).

Column Type	Rotational Spring Stiffness (kNm/rad)
MRF (Upper Limit)	55674.0
MRF (Intermediate)	33337.7
CBF (Upper Limit)	4952.0
CBF (Intermediate)	2965.3
Gravity (Lower Limit)	97.5

3.3. Column Connection Methods

Connecting the defined columns together was necessary as the intention of the model was to later generate the complete building system response under dynamic (scaled strong motion record) loading. The representative nature of the model meant that full physical features of every single structural element present within the Te Puni building were not individually stipulated. Hence, the method of connecting these columns to closely exhibit interactional behaviour between the column types required careful definition. The manner in which these links or connecting elements were specified within the model was made so as not to interfere with the analysis of the building, unless an expected effect such as presence of slabs were to be applied and captured. For the purposes of this 10-storey model, rigid longitudinal links and rigid members were considered the most appropriate linking elements.

3.3.1. Rigid Longitudinal Links

The most effective element to use was a simple rigid link between the nodes of the adjacent column at each storey of the building. Links allow for specialised structural behaviours relating to axial, shear, pure bending and torsional tendencies to be captured. However, the main function for these links was to provide a stiff and rigid connecting element so that interaction between the CBF and the gravity column would be represented when the system undergoes NLTHA. This means that the rigid longitudinal links, i.e., the green-coloured links between the gravity and CBF columns, represent the rigid diaphragm behaviour keeping the lateral displacement between the columns constant.

The link properties were set as linear with fixed U1 or horizontal directional properties. Not only were they appropriate to join the CBF and gravity columns within the model together, they possessed relevant characteristics to create a box detail which would be used to represent the SHJ component further on in the modelling process.

3.3.2. Rigid Members

Slab effect is identified as an important parameter of interest regarding self-centring capabilities. Floor slabs provide an extra element of additional stiffness to the overall building at each level. In practice, buildings will have slabs which will give rise to this effect where it should be encapsulated between the MRF and CBF representative columns. While rigid longitudinal links were also appropriate

in the case of no slab effect being examined, it does not allow for providing any properties to capture slab behaviour when it is present.

The best way to represent the slab effect was to capture it through partial end fixity springs between the column face of the MRF and the inter-column connecting element, hence exhibiting the resistance to rotation between the slab and the column and embodying restoring energies. These partial end fixity springs cannot be defined on rigid longitudinal links; however, the limitation was overcome by instead defining a rigid member which was set to very high stiffness and zero weight. Gridlines were defined to set up a node at a position where the column flange is expected to terminate on the side closest to the CBF column. Rigid members were then defined as shown in Figure 4, which also highlights the partial fixities on all ends of the rigid members for clarity.

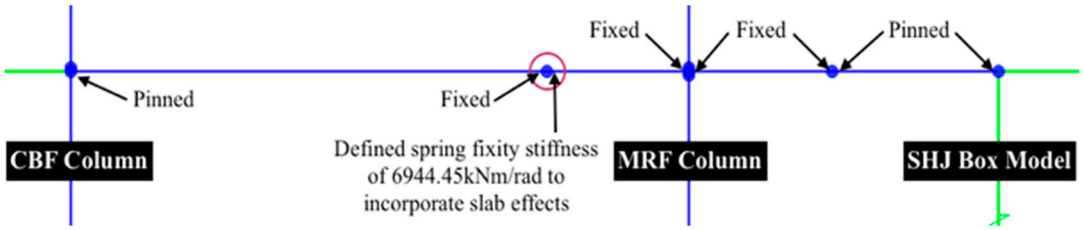

Figure 4. Rigid member partial fixity restraint conditions.

Previous research by [16] has been undertaken where force-deflection data was attained to capture the out of plane response of the composite slab with an Eccentrically Braced Frame (EBF) link. Despite not having EBFs in the current Te Puni building, the behaviour of the slab under dynamic conditions is expected to be sufficiently similar to be incorporated within the model. The spring values were therefore calculated using force and displacement averages attained from [16]. The particular tested EBF link was 0.8 m in length and a force of 75 kN was identified to produce an average deflection of 54 mm across the four tested mesh types. The moment and rotation which capture the slab effect, can therefore be calculated and then the spring constant representing each slab under consideration may also be calculated. Since there are ten slabs on each storey across the two MRFs which needed to be accounted for, a multiplier of 10 was applied to spring fixity values prior to SAP2000 input. This amounts to a partial spring fixity of 6944.45 kNm/rad on each of the ten floors within the building.

3.4. Sliding Hinge Joints

The simplistic manner in which the SHJ detail at each floor was modelled utilised the same rigid longitudinal links defined for inter-column connection. Additional gridlines were set up to the right of the MRF representative column as the interaction between the two remained a crucial aspect for accurate representation of the system. These were placed 0.5 m and 1 m away from the MRF column, and in combination with the top flange and bottom flange gridlines which were previously defined for each storey, a SHJ box detail was modelled as shown in Figure 5. A detailed explanation on the approach used to calculate the frictional resistance of the AFCs-represented links may be found in [6]. Moreover, detailed explanations of the seismic behaviour of the SHJ, as well as the sliding behaviour of the AFC, are presented in [5,17].

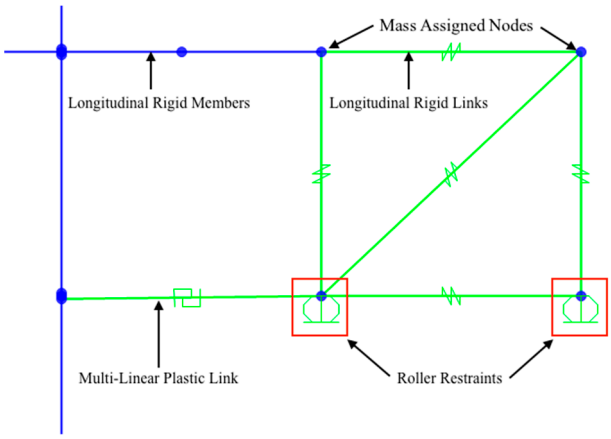

Figure 5. SHJ box-shaped model.

Roller restraints were applied to the bottom which allowed for horizontal movement and only restricted U3 vertical motion to allow the sliding mechanism to function. The top two nodes on the SHJ detail each had half of the total seismic weights assigned for the corresponding floor to encapsulate the system weight which was previously ignored in the modelling process. It is worth noting that the green-coloured longitudinal rigid links are used to make it possible to define and model 1) the geometrical characteristics of the SHJ, such as beam's depth, 2) the roller restraints to allow the lateral displacement and column-beam relative rotation and AFC sliding, and 3) the seismic lumped mass nodes. These longitudinal rigid links are not deformable structural elements, but just displacement restraints, and hence do not increase the computational cost of running the model.

3.4.1. Backbone Curve Definition

The top of the SHJ detailing was connected using rigid members in a similar manner to the inter-column CBF to MRF connection. This provided a good representation of the rotational mechanism on the top flange with pinned releases where the sliding mechanism at the bottom would simply cause rotation to occur about the connecting point of the top flange plate and the column flange. However, the frictional connection properties relating to how the detail performs under dynamic conditions needed to be defined using a special link connecting the bottom of the connection to the MRF representative column centreline.

A spreadsheet was set up to define the link properties of SHJ at each level using the method described in [4] for predicting the sliding shear capacities (V_{SS}) using plastic theory-based bolt model equations. The stable sliding bolt tension (N) was extracted from Table 1 of [4] according to a cleat thickness of 16 mm for all SHJs up the building, as well as the respective bolt sizes which were used for the connection component considered [4]. It was identified that only four new links with varying V_{SS} had to be defined for the building, as some storeys had the same SHJ bolt compositions for the web and bottom flange sliding components. These four links were categorised for Level 4–8, Level 9–10, Level 11–12 and Level 13. It is worth noting that the first storey above ground level is Level 4, increasing numerically to Level 13, which is the top storey considered in the model.

It was necessary to distinguish the V_{SS} from the bottom web component and from the bottom flange component of the AFC separately as they function at different lever arms to the point of rotation, due to the location of the bolts. For clarity, V_{SS} provided by the web component was considered F_1 while V_{SS} provided by the flange component was considered F_2. To find the total combined V_{SS} provided by either component, the same equation was used, $V_{SS} = 2 \times \mu \times N \times B$, which accounted for a coefficient of friction (μ) of 0.5 [17] and the number of bolts which contributed to that component (N), and the clamping force (bolt tension) delivered by each bolt (B). The capacity was seen to be multiplied by two to account for the two frictional surfaces which will be initiated in sliding.

Based on the as-designed connection layout regarding the vertical positioning of the bolt centrelines in relation to the point of rotation, the relative contribution of the bottom web bolts was considered to be 83% of its calculated capacity as taken from research conducted by [6]. For the bottom flange bolts, the contribution remained full at 100%, as this was the initial condition from which the V_{SS} was calculated. The sum of these two components then produced sliding capacities for each SHJ with AFC at the storey of interest.

As the model joint at each level represents the SHJ behaviour across the entire storey, the input values into the link properties must consider the total number of SHJs present at that level. This amounted to 20 across the two MRFs in the building, which can be seen as the total V_{SS} for the level in Table 2.

Table 2. Shear sliding capacity contribution breakdown.

SHJ	F_1 (kN)	F_2 (kN)	V_{SS} Total Per Storey (kN)
Level 4-8	381.2	508.2	16491.1
Level 9-10	244.0	488.0	13809.8
Level 11-12	244.0	325.3	10556.6
Level 13	140.3	187.1	6072.0

The total V_{SS} at each level was defined to occur at a displacement of 0.01 mm at which sliding was considered to initiate, and up to 20 mm of deformation for both positive and negative directions was expected, as exemplified in Figure 6. This interval reflects the likely range expected in a severe earthquake in practice [6]. Effective stiffness values were attained considering that the total V_{SS} at the level will cause a displacement of 0.01 mm in the plastic region, while effective damping was assumed to be at 0.05x critical. It is worth noting that a more practical and realistic value of the displacement associated with the initiation of the sliding may be 0.1 mm not 0.01 mm, as is explained in [6].

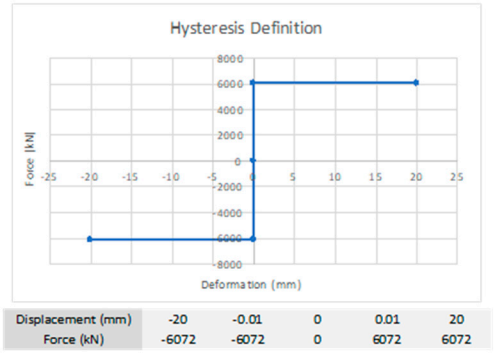

Figure 6. Hysteresis definition for Level 13 SHJ links.

The definition of the links incorporating the SFC hysteresis used the same methodology and total V_{SS} values calculated for AFC.

3.4.2. SAP 2000 Hysteresis Selection

The link itself was defined with multilinear plastic properties, where the U1 horizontal direction was assigned as non-linear so a hysteresis could be established. The idealised moment-rotational hysteresis which represents the entirety of conventional AFC behaviour is shown in Figure 7 [18].

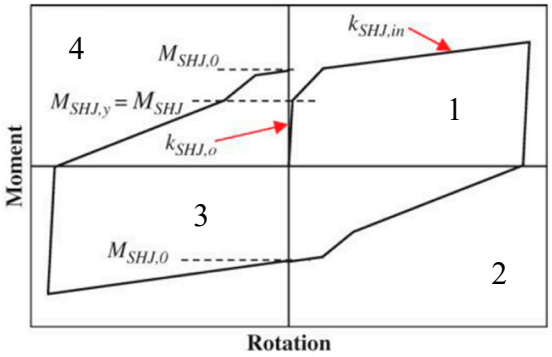

Figure 7. SHJ with conventional AFC behaviour spine curve [18].

Time and resource limitations have not yet enabled a single hysteresis type that best captures a non-optimised AFC detail to be established (this work is underway in 2019). Hence, SAP pre-defined hysteresis curves were used for this research. In terms of pre-set hysteresis types without need for additional input parameters, the behaviour of the SHJs with AFC or SFC during an earthquake and its expected force-deformation features was expected to be most closely associated with the Isotropic Hysteresis Curve (IHC), the Kinematic Hysteresis Curve (KHC) or the Takeda Hysteresis Curve (THC). These curves have different implications to the main outputs of interest, namely, the maximum displacements and the residual drifts.

The maximum drift envelope is principally controlled by the resistance to increasing deformation as shown in the 1st and 3st quadrants of Figure 7. It shows that conventional AFCs have high strength to embody this effect, and no degradation in strength is expected in these two quadrants with successive cycles of loading. This is best captured by the SAP hysteresis elastoplastic curves with either kinematic or isotropic hardening (KHC or IHC). Typically, the magnitude of deformations is somewhere between the results given by these two curves. Therefore, these curves were used to obtain the maximum drift response.

The residual drift, however, is principally controlled by the characteristics in the 2nd and 4th quadrants. It is measured by how easily the joint returns to zero rotation from positive or negative rotation in these quadrants. For the SHJ with AFC, moments generated in these quadrants by the KHC or the IHC curves are very significantly overestimated, meaning that residual drifts would not be accurate. Of the three hysteresis curves used, the THC was a suitable choice for this purpose. However, the THC was expected to significantly understate the resistance to deformation due to its behaviour in the 1st and 3rd quadrants, deeming it less appropriate for maximum drift determination, which it will overestimate.

While the Te Puni building being modelled is constructed with AFC detailing, SFC detailing has been more widely used and researched in other parts of the world. Therefore, it was of interest to capture SFC behaviour for comparative reasons within the results obtained from NLTHA. The major difference was the hysteresis shape which best reflects the behaviour of the detail as the building undergoes dynamic movement. The IHC is expected to most accurately capture SFC tendencies.

3.5. Extra Considerations

Prior to running the model for results, accurate application of the gravity loads onto each storey of the gravity column was required. This allowed the NLTHA to incorporate second-order P-Delta effects, which realistically would influence the drift of the building. Through the use of un-factored self-weight permanent, imposed, and super-imposed permanent loads extracted from the calculation set, a seismic weight load case was applied to tributary areas for the gravity columns in accordance to [19]. This was used to calculate a point load of 604.35kN, placed on the node of each storey on the representative compound gravity column.

The second consideration before running the model was to prepare three additional models with different columns and features present. This enabled the effect on the displacement and drift values when new components are added or taken away to be quantified through running NLTHA on each copy. The prescribed methodology highlighted the development of a full building model for the purposes of this research. However, these three other models were easily obtained from this base copy.

The first altered model was a whole building model without the slab effect which could be formed by setting the rotational spring between the rigid members as specified in Section 3.3.2 to zero, thus initiating a pinned effect. The second altered model with only CBF and MRF present involved the removal of the gravity column and the links which connected it to the CBF column. The final altered model with only the MRF was created from removing the CBF column and also all rigid members which connected it to the MRF column.

4. Selection of Earthquake Time-History Record

To select an appropriate past earthquake time-history record, the method established in [20] was implemented. This resulted in the El Centro 1940 earthquake record being an appropriate record to apply to the model. Three levels of earthquake were considered; Serviceability Limit State (SLS), Ultimate Limit State (ULS) and Maximum Considered Event (MCE), which are associated with return periods of 25, 500, and 2500 years, respectively, for this "normal importance" building. These different levels of earthquake were scaled in accordance to [19]. Because of the project deadline, only one record could be run.

4.1. Non-Linear Time History Analysis (NLTHA)

4.1.1. Modal Case

Eigen Vectors were used for the modal case in SAP2000. For Eigen Vectors, the starting load vectors needed to be defined and these were: acceleration in x-direction (along the frame), the load pattern for the model including the gravity column, and the built-in deformation mode for the links.

4.1.2. Direct Integration Nonlinear Analysis (DINA)

DINA was chosen as another NLTHA because of its accuracy for both the deflection envelope and residual displacement data. This analysis can also consider second order effects from geometric non-linearity which are often referred to as P-delta effects. These effects are the additional deflection demands that result when the structure is deflected from its natural position and the axial load on the column is now acting at a lever arm. It is important to consider any additional deflection demands to produce the most accurate data possible. The limitation of a DINA is that it requires significant computational time, which is a matter of hours.

To realistically capture the response of the structure for the models including the gravity column, the starting condition of the earthquake cases (SLS, ULS and MCE) needed to be defined as a non-linear static load case using modes from modal case. This is because the models that have the representative gravity column in them have loads applied at each storey along the column. When defining this load case to account for the P-delta effects explained earlier, "P-Delta plus Large Displacements" was selected.

The DINA load case is a non-linear direct integration time history using modes from the modal case. To account for the P-delta effects in this load case, "P-Delta plus Large Displacements" was also selected. For the models including the gravity column this case starts from the conclusion of the load case for the loads on the gravity column. There were also three DINA load cases undertaken, which corresponded to the three levels of earthquake investigated. The time increment used was 0.002 seconds used for 31,750 output time steps to cover the duration of the El Centro 1940 earthquake record data.

4.2. Damping

Damping is an important parameter to incorporate in a non-linear analysis because it represents the efficiency of the structure to dissipate the energy input from an action, which in this case is the earthquake. The elastic damping is required to mathematically implement the dynamic equation of motion. A value of 5% elastic damping may be the most appropriate value associated with the mode of vibration which has the largest mass participation. The mode with the largest mass participation from the model is mode one which comprises 84% of the participating mass. Mode one is the first mode of vibration of the multi-storey building in which the seismic masses, i.e., degrees of freedom, moves in the same phase.

Rayleigh damping was used in the model, but the challenge with Rayleigh damping is that it increases with frequency. The higher modes account for 16% of the participating mass. The participating mass of each mode is proportional to the extent of deformation associated with that mode. This means higher damping for these modes would under-represent their contribution to deformation. To overcome this, according to [21], the damping was to be taken as 5% at the period for mode 1 and 5% for the period associated with the mode number that is equal to the number of stories in the structure. This resulted in a 5% damping taken for the mode 1 with a period of 1.27 s and for mode 10 with a period of 0.07 s. The modes between modes 1 and 10 will therefore have damping values of below 5%, which is appropriate to avoid under representing their contribution.

5. Results/Analysis

5.1. Displacement

The maximum lateral displacements for the models during the ULS earthquake are shown in Table 3, below, for the Kinematic Hysteresis Curve (KHC) and Isotropic Hysteresis Curve (IHC) models.

Table 3. Maximum lateral displacement during ULS earthquake for KHC & IHC (mm).

Storey	Whole Building with Slab	Whole Building without Slab	MRF + CBF	MRF
13	135	138	137	136
12	129	131	130	130
11	117	119	118	118
10	99	101	100	100
9	83	84	84	83
8	72	72	72	71
7	64	65	64	64
6	50	51	50	50
5	40	41	40	41
4	24	25	24	25

The inclusion of the Takeda Hysteresis Curve (THC) in the model for the whole building with slab can be seen in Table 4.

The AFC models using the KHC produced identical displacement results to the SFC models using the IHC, and these are plotted in Figure 8 for the whole building with slab model. The displacement envelope for the AFC models using the THC produced a smaller deflection envelope than the KHC as seen in the plotted ULS case in Figure 8.

Table 4. Maximum lateral displacement for whole building with slab model including the THC for the ULS case.

Storey	Maximum Lateral Displacement (mm)
13	122
12	117
11	108
10	94
9	79
8	66
7	58
6	46
5	38
4	23

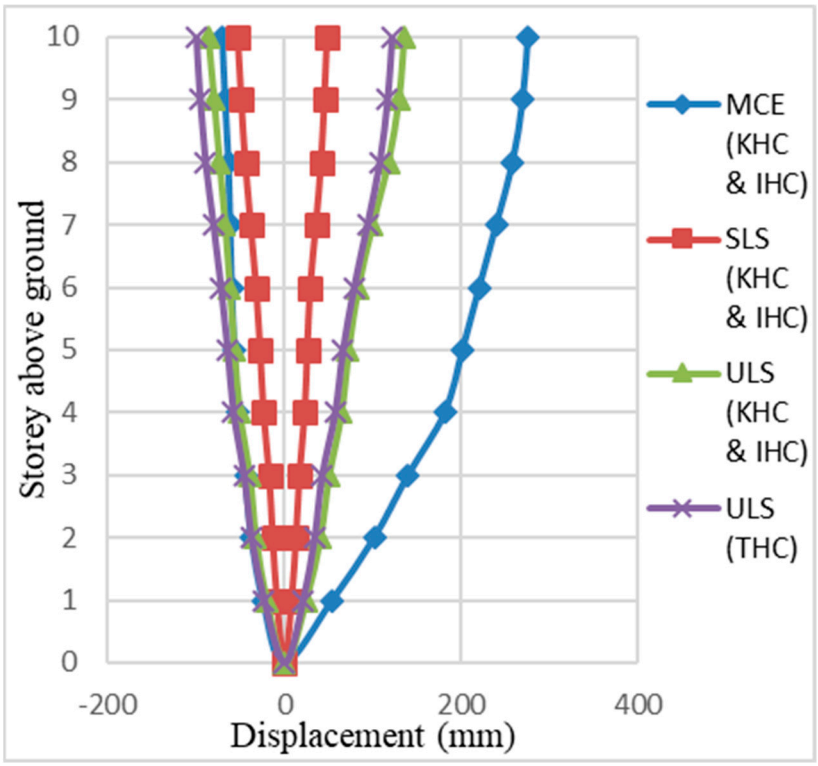

Figure 8. Displacement envelope for whole building with slab.

The New Zealand Seismic Loadings Standard NZS 1170.5 [19] states that the "ultimate limit state inter-storey deflection determined in accordance with Clause 7.3.1 shall not exceed 2.5% of the corresponding storey height". The ULS maximum inter-storey drift for the KHC and IHC models are shown in Table 5, below, and are all well below the 2.5% limit. It is worth noting that the maximum inter-storey drift for the KHC and IHC models for the MCE case were below 1.9% for all models, too

Table 5. Maximum inter-storey drift for KHC and IHC models for the ULS case (%).

Level	Whole Building with Slab	Whole Building without Slab	MRF + CBF	MRF
4	0.81	0.82	0.81	0.83

The model of the whole building with slab including the THC produces a maximum inter-storey drift of 0.78% at level 4 for ULS case, as seen in Table 6. This is well below the 2.5% limit.

Table 6. Maximum inter-storey drift for whole building with slab using THC for the ULS case.

Storey	Maximum Inter-Storey Drift (%)
13	0.13
12	0.30
11	0.47
10	0.50
9	0.42
8	0.26
7	0.30
6	0.29
5	0.48
4	0.78

5.2. Self-Centring Capabilities

For a building to be self-centring, its residual inter-storey drift needs to be within +/− 0.14%, which is the limit found to be satisfactory to avoid structural repair following the assessment of structures affected by the 2011 Christchurch earthquake [22]. The KHC and IHC produced the same residual drift values, and their results for the ULS case for the models are provided in Table 7.

Table 7. Residual inter-storey drift for KHC and IHC models for the ULS case (%).

Storey	Whole Building with Slab	Whole Building without Slab	MRF + CBF	MRF
13	0.02	0.02	0.02	0.02
12	0.10	0.10	0.10	0.10
11	0.17	0.19	0.19	0.19
10	0.16	0.18	0.18	0.18
9	0.11	0.12	0.11	0.11
8	0.03	0.03	0.03	0.02
7	0.04	0.04	0.04	0.04
6	0.02	0.02	0.02	0.02
5	0.04	0.04	0.04	0.04
4	0.08	0.09	0.09	0.09

Storeys 10 and 11 have residual inter-storey drift values above the +/− 0.14% limit for the KHC and IHC models. The addition of the CBF and gravity column do not make much difference to the residual inter-storey drift. When considering the influence of the slab, the residual inter-storey drift decreases for four of the storeys, including the 10th and 11th storey. Though the slab decreases the residual inter-storey drift for storeys that exceed the limit, this reduction is not enough for the storey drift to be within the limit.

The residual inter-storey drift for THC models produce much smaller values than the KHC and IHC models. This can be seen in Table 8 with a maximum value of +/− 0.04% in the ULS case occurring in storeys 4 and 10.

Table 8. The THC residual displacement and inter-storey drift for the ULS case.

Storey	Residual Displacement (mm)	Residual Inter-Storey Drift (%)
13	3	0.00
12	3	0.01
11	2	0.03
10	1	0.04
9	0	0.02
8	−1	−0.01
7	−1	0.00
6	−1	0.00
5	−1	0.00
4	−1	−0.04

The results for the KHC, IHC and THC deformation results are shown in Tables 9 and 10. This data is representative of what happens in the SHJ's friction connection details during and after earthquake.

Table 9. KHC and IHC deformation results for whole building with slab model in ULS case.

Storey	Deflection Envelope (mm)		Residual Deflection (mm)	Maximum Deflection/ Residual Deflection
13	−0.05	0.07	0.00	20.19
12	−0.07	0.09	0.01	8.07
11	−0.48	1.22	0.73	1.68
10	−0.05	0.69	0.59	1.17
9	−0.06	0.98	0.84	1.17
8	−0.04	0.14	0.05	3.06
7	−0.04	0.31	0.21	1.48
6	−0.08	0.30	0.20	1.51
5	−0.19	0.71	−0.08	−8.68
4	−1.40	2.00	0.45	4.42

Table 10. THC deformation results for whole building with slab model in ULS case.

Storey	Deflection Envelope (mm)		Residual Deflection (mm)	Maximum Deflection/ Residual Deflection
13	−0.06	0.06	0.00	174.87
12	−0.08	0.08	0.00	65.14
11	−0.71	1.08	0.09	11.83
10	−0.06	0.52	0.18	2.94
9	−0.06	0.89	0.24	3.71
8	−0.06	0.14	0.03	5.43
7	−0.07	0.22	0.06	3.98
6	−0.09	0.12	0.01	15.08
5	−0.48	0.38	−0.04	11.86
4	−1.79	1.43	−0.07	26.18

The THC results showed a maximum residual deflection of 0.24 mm occurring at the 9th storey, while KHC and IHC had a maximum value of 0.84 mm occurring at the 9th storey. The average maximum ratio of deflection to residual deflection was 3.41 and 32.1 for KHC/IHC and THC, respectively.

5.3. Column Base Rotational Stiffness

The base rotational stiffness was reduced for the MRF and CBF column bases, which were all effectively pinned column bases, to an intermediate pinned base value. This reduced value was considered to investigate the influence of the column base rotational stiffness in a range that represents a pinned column base. In Tables 11 and 12, below, are the results for the whole building with slab model in the ULS case for the three different hysteresis curves.

When reducing the column base fixity, in a range representing pinned column bases, the following was found for the ULS case, as seen in Tables 11 and 12, when compared to the results shown in Tables 3–8:

- The maximum lateral displacement changed for all three hysteresis curves. The maximum lateral displacements decreased at the upper storeys and then increased at the lower storeys with a few storeys unchanged in the middle. The maximum change was a 2 mm difference and most of the changes were +/− 1 mm.
- The maximum inter-storey drift found on the 4th storey increased by 0.02% for the KHC and IHC models.
- The maximum inter-storey drift found on the 4th storey increased by 0.03% for the THC models.

- The residual inter-storey drift for the KHC and IHC still failed the +/− 0.14% limit on the 10th and 11th storeys. The value decreased for the 11th storey from 0.17% to 0.16%.
- The maximum residual inter-storey drift for the THC models stayed the same at +/− 0.04% for storeys 4 and 10. This is well below the recommended limit.

Table 11. Results from reduced rotation base stiffness for the whole building with slab model including KHC and IHC for the ULS case.

Storey	Maximum Lateral Displacement (mm)	Maximum Inter-Storey Drift (%)	Residual Inter-Storey Drift (%)
13	134	0.16	0.02
12	128	0.38	0.09
11	116	0.59	0.16
10	99	0.53	0.16
9	83	0.38	0.11
8	71	0.25	0.02
7	64	0.34	0.03
6	50	0.32	0.02
5	41	0.52	0.04
4	25	0.83	0.09

Table 12. Results from reduced rotation base stiffness for the whole building with slab model including THC for the ULS case.

Storey	Maximum Lateral Displacement (mm)	Maximum Inter-Storey Drift (%)	Residual Inter-Storey Drift (%)
13	120	0.13	0.00
12	115	0.29	0.01
11	107	0.46	0.03
10	93	0.49	0.04
9	78	0.41	0.01
8	66	0.23	−0.02
7	59	0.30	0.00
6	47	0.28	0.00
5	39	0.48	0.00
4	24	0.81	−0.04

6. Discussion

6.1. Self-Centring Capability

The use of the IHC for SFC and KHC for AFC produced identical results, which brought up the question as to whether the KHC is the most appropriate AFC hysteresis curve. This is because the AFC should produce smaller residual drift results than the SFC. The hysteresis curves for the 11th storey, same model and ULS case are plotted below for IHC and KHC models. The hysteresis curves are identical to those seen in Figures 9 and 10. The curves follow the expected shape for the SFC hysteresis curve.

The THC for the same case as the KHC and IHC above is plotted in Figure 11.

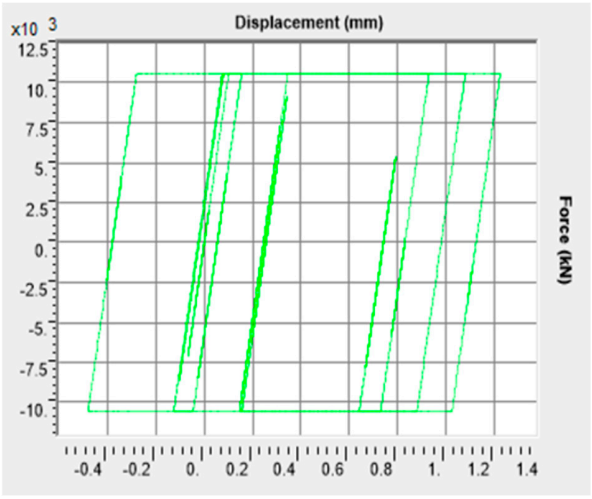

Figure 9. Hysteresis curve for whole building with slab model at 11th storey for KHC model in the ULS case.

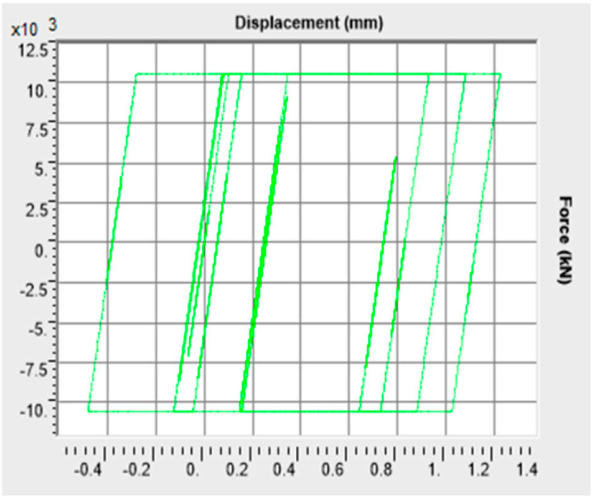

Figure 10. Hysteresis curve for whole building with slab model at 11th storey for IHC model in the ULS case.

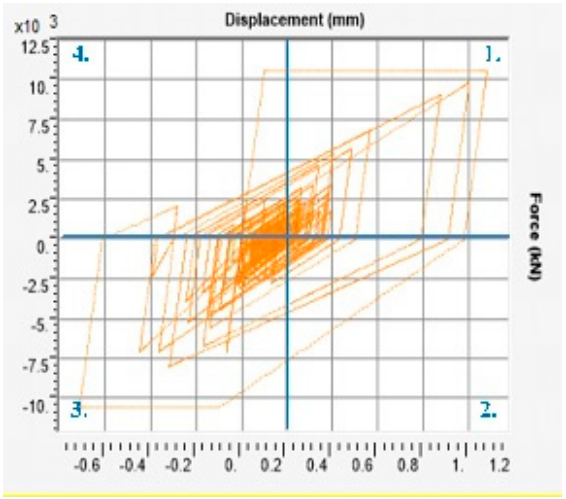

Figure 11. Hysteresis curve for whole building with slab model at 11th storey for the THC model in the ULS case.

In the 2nd and 4th quadrants of Figure 11, the area is less occupied than the 2nd and 4th quadrants in Figures 9 and 10, which is due to the lowering of resistance to sliding that brings the building back to centre more effectively. This is more representative of the behaviour of the AFC and is reflected in the low residual drift values we would expect when implementing the AFC. For this reason, the THC models produce the most representative residual drift values for the AFC. The residual inter-storey drift values for the THC AFC are well below the limit of +/− 0.14%, meaning the AFC provides sufficient self-centring capabilities.

From these results, the AFC produces significant improvements in the self-centring capabilities of a building in comparison to the SFC. The KHC and THC are not a perfect representation of the AFC response and due to time restrictions, a perfect hysteresis curve for the AFC was not attainable, and a more representative hysteresis curve would require further research. The optimised AFC with BeSs [10] is expected to perform better than the original AFC, but further research needs to be undertaken to attain an accurate hysteresis curve of the optimised AFC.

The IHC residual drift from the models is most appropriate for the SFC as the hysteresis curve in Figure 9 confirms the expected result for the SFC. This means the SFC has shown to not provide sufficient self-centring capabilities as the residual inter-storey drift exceeds the limit of 0.14%. This suggests that SFC might not be a good low damage solution in terms of self-centring.

The greater the ratio of maximum deflection/residual deflection shows greater effectiveness of the friction sliders (as part of the whole system) in dissipating energy and at the same time their high tendency to come back to their original position (self-centre). The THC shows a tenfold increase in the average ratio across all storeys when compared to the KHC and IHC data.

The additional representative columns had a negligible effect on the residual inter-storey drift. The inclusion of the slab effects reduced the residual inter-storey drift. This was particularly noticeable on the storeys that had the largest residual inter-storey drift before including the slab effects.

6.2. Lateral Displacements

The maximum lateral displacement at each storey increased when additional representative columns were added to the model. The gravity load on the gravity column would initiate P-Delta effects which are incorporated in the DINA which could partly explain this result. It is important to note that the mass multipliers for the additional columns were set to zero, so no additional mass was added to the model which could have explained this result. The natural frequency changes with the additional representative columns which could indicate the natural frequency is getting closer to the governing frequency content of the earthquake record. This potentially explains the increase in maximum lateral displacement at each storey, but analysis with a wider range of earthquake records would be required to confirm this. The model of the whole building showed a decreased maximum lateral displacement when incorporating the effects of the slab which is to be expected in practice due to the increased stiffness that the slab contribution adds to the building.

The Takeda hysteresis curve in Figure 11 shows degradation in the 1st and 3rd quadrants, which means the structure has already slightly softened before the peak demand cycle arrives. This explains why the peak deflection values are slightly smaller in the THC models than the KHC and IHC models for the same model and load case as seen in Tables 3 and 4. In practice the SHJ with AFC or SFC does not degrade in stiffness over multiple cycles which means the KHC and IHC deflection envelopes are most appropriate for the AFC and SFC respectively.

The ULS inter-storey drifts are within the limit of 2.5% for all four models and all three hysteresis curves, which suggests that inter-storey deflection is not an issue when implementing SFC or AFC connection details in SHJs.

6.3. Column Base Rotational Stiffness

Reducing the base fixity to a value closer to that of a perfectly pinned column base has had very little effect on the maximum inter-storey deflection, maximum inter-storey drift, and residual

inter-storey drift. This is encouraging, as this suggests that a great amount of detail does not need to be used to find the exact base fixity found in practice for a pinned column base. It is worth noting that from the self-centring point of view (i.e., residual drift), a rigid column base (either 1.67EI/L or 1.0EI/L of column base rotational stiffness) kept in the elastic range makes the tendency of the building to self-center significantly higher, and the maximum drift may also be smaller. These can be easily investigated through further parametric study using the proposed simplified numerical model.

6.4. General Comments

The simple model developed can be used for future research to compare and quantify the response of different types of friction connections and connections in general.

Further research would need to be undertaken to account for the effects of non-structural elements as well as practical column base fixities.

There are no recommendations required for the AFC, as there is no need to minimise post-earthquake residual drift. It is recommended for the SFC that the post-earthquake residual drift is minimised by increasing column in-plane strength/stiffness or potentially by implementing springs if there is really a need. A detailed discussion on the use of such springs may be found in [6].

7. Conclusions

The principal conclusions from this study are as follows:

- A simplified multi degree of freedom model of the 13-storey Te Puni building was successfully created in SAP 2000.
- The inter-storey drift for all four models and three hysteresis curves analysed in the ultimate limit state were well below the code-specified 2.5% limit, even with the MRFs with pinned column base and gravity columns with perfectly pinned column base.
- Maximum lateral displacement increased with additional representative columns, which is suggested to be accredited to the influence of P-Delta effects and/or the natural frequency of the models getting closer to the governing frequency of the earthquake record. This may need to be investigated further through further parametric study using the proposed simplified numerical model.
- The isotropic hysteresis curve produced identical data to the kinematic hysteresis curve when implemented in the models.
- The isotropic hysteresis curve is appropriate for the symmetrical friction connection.
- The kinematic hysteresis curve produces more representative deflection envelope displacement for the asymmetric friction connection than the Takeda hysteresis curve.
- The Takeda hysteresis curve produces more representative residual displacements for the asymmetric friction connection than the kinematic hysteresis curve.
- The residual drift for the symmetric friction connection that used the isotropic hysteresis curve exceeded the +/− 0.14% limit for the ultimate limit state, which suggests that the connection might not be an ideal low damage solution in terms of self-centring capability; however, the influence of the non-structural elements, such as walls, and more importantly the influence of the practical column base fixities which are effectively fixed for the MRFs and designed to behave elastically, still need to be studied to comprehensively explain the actual seismic behaviour of the building, which is expected to be significantly enhanced.
- The residual drift for the asymmetric friction connection that used the Takeda hysteresis curve was well below the +/− 0.14% limit for the ultimate limit state, hence suggesting an overall system that exhibits dynamic self-centring at system level, even with the MRFs with pinned column base and gravity columns with perfectly pinned column base.
- Including the additional representative columns with effectively pinned column base had negligible effect on the residual inter-storey drift.

- Including the influence of the slabs effect reduced the residual inter-storey drift. This was particularly noticeable on the storeys that had the largest inter-storey drift before including the slab effects and is similar to the findings from [16].
- Reducing the base fixity to a closer value to that of a perfectly pinned column base has had very little effect on the maximum inter-storey deflection, maximum inter-storey drift, and residual inter-storey drift. However, from the self-centring point of view (i.e., residual drift), a rigid column base (either 1.67EI/L or 1.0EI/L of column base rotational stiffness) kept in the elastic range makes the tendency of the building to self-centre significantly higher, and the maximum drift may also be smaller. These can be easily investigated through further parametric study using the proposed simplified numerical model.

Author Contributions: Conceptualization, S.R. and G.C.C.; Methodology, S.R. and G.C.C.; Software, S.R., G.C.C., M.L. and G.A.M.; Validation, S.R., G.C.C. and M.L.; Formal analysis, S.R., G.C.C., M.L. and G.A.M.; Investigation, S.R., G.C.C., M.L. and G.A.M.; Resources, S.R. and G.C.C.; Data curation, S.R., G.C.C., M.L. and G.A.M.; Writing—original draft preparation, S.R.; Writing—review and editing, S.R. and G.C.C.; Visualization, S.R., G.C.C., M.L. and G.A.M.; Supervision, S.R. and G.C.C.; Project administration, S.R., G.C.C. and M.L.; Funding acquisition, S.R. and G.C.C.

Funding: The Financial supports from the Earthquake Commission Research Foundation (EQC) (Project 14/U687 "Sliding Hinge Joint Connection with BeSs"), NZ Centre for Earthquake Resilience (QuakeCoRE), and Heavy Engineering Research Association (HERA) are much appreciated.

Acknowledgments: Advice from Quincy Ma of the University of Auckland (UoA) regarding the time history analysis is also appreciated. The The authors would like to also thank the UoA final year BSc students Travis Good and Shirley Jiang who helped in making the numerical model as their final year projects.

Conflicts of Interest: The authors declare no conflict of interest.

References

1. Ramhormozian, S.; Clifton, G.C.; Good, T.; Jiang, S.; MacRae, G.A. Dynamic Time History Analysis of a Low Damage Multi-Storey Building Incorporating the Seismic Friction Dampers using a Proposed Simplified Multi Degree of Freedom (MDOF) Model: Is Self-centring Really a Concern? In Proceedings of the Pacific Conference on Earthquake Engineering, Auckland, New Zealand, 4–6 April 2019.
2. Hollings, J.P. *Reinforced Concrete Seismic Design*; Bulletin of the New Zealand Society for Earthquake Engineering: Wellington, New Zealand, 1968; pp. 217–250.
3. Ramhormozian, S.; Clifton, G.; English, S.; Fredheim, S.; Beskhyroun, S.; Macrae, G. Dynamic Performance Analysis and System Identification (SI) of a Low Damage Multi-Storey Structural Steel Building under two Moderately Severe Earthquake Events using Structural Health Monitoring (SHM) Data. In Proceedings of the NZSEE Annual Technical Conference, Auckland, New Zealand, 13–15 April 2018.
4. Ramhormozian, S.; Clifton, G.; MacRae, G. The Asymmetric Friction Connection with Belleville springs in the Sliding Hinge Joint. In Proceedings of the New Zealand Society for Earthquake Engineering (NZSEE) Annual Technical Conference, Towards Integrated Seismic Design, Auckland, New Zealand, 21–23 March 2014.
5. Ramhormozian, S.; Clifton, G.C.; MacRae, G.A.; Davet, G.P. Stiffness-based approach for Belleville springs use in friction sliding structural connections. *J. Constr. Steel Res.* **2017**, *138*, 340–356. [CrossRef]
6. Ramhormozian, S.; Clifton, G.C.; Takayama, Y.; Lam, J.; Macrae, G. Self-Centering Capability of the Seismic Friction Dampers: A Conceptual Study on the Static and Dynamic Self-Centering Requirements for the Single Degree of Freedom (SDOF) Asymmetric and Symmetric Friction Connections (AFC and SFC)Zealand. Presented at the New Zealand Society for Earthquake Engineering Annual Conference, Wellington, New Zealand, 2017.
7. Clifton, G.C. Semi-rigid Joints for Moment-Resisting Steel Framed Seismic-Resisting Systems. Ph.D. Thesis, Department of Civil and Environmental Engineering, University of Auckland, Auckland, New Zealand, 2005.
8. Ramhormozian, S.; Clifton, G.C.; MacRae, G.A.; Khoo, H.H. The Sliding Hinge Joint: Final Steps towards an Optimum Low Damage Seismic-Resistant Steel System. *Key Eng. Mater.* **2018**, *763*, 751–760. [CrossRef]

9. Ramhormozian, S.; Clifton, G.C.; Bergen, B.; White, M.; Macrae, G.A. An Experimental Study on the Asymmetric Friction Connection (AFC) Optimum Installed Bolt Tension. In Proceedings of the NZSEE Annual Technical Conference and 15th World Conference on Seismic Isolation, Energy Dissipation and Active Vibration Control of Structures, Wellington, New Zealand, 27–29 April 2017.
10. Ramhormozian, S. *Enhancement of the Sliding Hinge Joint Connection with Belleville Springs*; University of Auckland: Auckland, New Zealand, 2018.
11. Chancellor, N.B.; Eatherton, M.R.; Roke, D.A.; Akbaş, T. Self-centering seismic lateral force resisting systems: High performance structures for the city of tomorrow. *Buildings* **2014**, *4*, 520–548. [CrossRef]
12. Lao, Y.P. *Floor Slab Influence on the Seismic Behaviour of a Concentrically Braced Frame with Stepping Base*; University of Auckland: Auckland, New Zealand, 2012.
13. Gledhill, S.; Sidwell, G.; Bell, D. The damage avoidance design of tall steel frame buildings—Fairlie terrace student accommodation project. In Proceedings of the 2008 New Zealand Society for Earthquake Engineering, Victoria University of Wellington, Wellington, New Zealand, 11–13 March 2008.
14. Gledhill, S.; Sidwell, G.; Khoo, H.H.; Clifton, G.C. Steel Moment Frames with Sliding Hinge Joints—Lessons Learnt During Implementation. In Proceedings of the Steel Innovations Conference, Christchurch, New Zealand, 21–22 February 2013.
15. NZS3404. *Steel Structures Standard, Incorporating Amendments 1 and 2*; Standards New Zealand: Wellington, New Zealand, 2007.
16. Momtahan, A. *Effects of Out of Plane Strength and Stiffness of Composite Floor Slabs on the Inelastic Response of Eccentrically Braced Frame*; University of Auckland: Auckland, New Zealand, 2015.
17. Ramhormozian, S.; Clifton, G.C.; MacRae, G.A.; Davet, G.; Khoo, H.-H. Experimental Studies on Belleville Springs use in the Sliding Hinge Joint Connection. *J. Constr. Steel Res.* **2019**, *159*, 81–94. [CrossRef]
18. Khoo, H.-H.; Clifton, C.; Butterworth, J.; MacRae, G. Experimental study of full-scale self-centering sliding hinge joint connections with friction ring springs. *J. Earthq. Eng.* **2013**, *17*, 972–997. [CrossRef]
19. NZS1170.5:2004. *Structural Design Actions—Part 5: Earthquake Design Actions*; Standards New Zealand: Wellington, New Zealand, 2004.
20. Oyarzo-Vera, C.A.; McVerry, G.H.; Ingham, J.M. Seismic zonation and default suite of ground-motion records for time-history analysis in the North Island of New Zealand. *Earthq. Spectra* **2012**, *28*, 667–688. [CrossRef]
21. Carr, A.J. *Ruaumoko Manual*; University of Canterbury: Christchurch, New Zealand, 2007.
22. Clifton, G.C. Lessons Learned for Steel Seismic Design from the 2010/2011 Canterbury Earthquake Series. In Proceedings of the Australian Earthquake Engineering Society 2013 Conference, Tasmania, Australian, 15–17 November 2013.